Accepted Manuscript

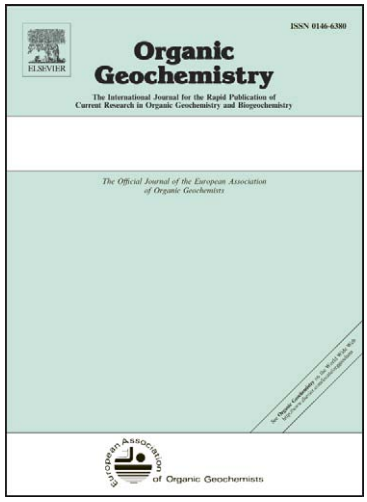

Simulation of soil organic carbon response at forest cultivation sequences using ^{13}C measurements

Pia Gottschalk, Jessica Bellarby, Claire Chenu, Bente Foereid, Pete Smith, Martin Wattenbach, Shamie Zingore, Jo Smith

PII: S0146-6380(09)00100-4
DOI: 10.1016/j.orggeochem.2009.04.017
Reference: OG 2352

To appear in: *Organic Geochemistry*

Received Date: 23 November 2008
Revised Date: 10 April 2009
Accepted Date: 30 April 2009

Please cite this article as: Gottschalk, P., Bellarby, J., Chenu, C., Foereid, B., Smith, P., Wattenbach, M., Zingore, S., Smith, J., Simulation of soil organic carbon response at forest cultivation sequences using ^{13}C measurements, *Organic Geochemistry* (2009), doi: 10.1016/j.orggeochem.2009.04.017

Simulation of soil organic carbon response at forest cultivation sequences using ^{13}C measurements

Pia Gottschalk[1], Jessica Bellarby[1], Claire Chenu[2], Bente Foereid[1], Pete Smith[1], Martin Wattenbach[1], Shamie Zingore[3], Jo Smith[1]

[1] *Institute of Biological and Environmental Sciences, School of Biological Sciences, University of Aberdeen, Cruickshank Building, St Machar Drive, Aberdeen, AB24 3UU, UK*

[2] *INAPG, UMR Bioemco, Bâtiment EGER, 78850 Thiverval Grignon, France*

[3] *Tropical Soil Biology and Fertility Institute of CIAT, Chitedze Research Station, Box 158, Lilongwe, Malawi*

Correspondence: Pia Gottschalk, Institute of Biological and Environmental Sciences, School of Biological Sciences, University of Aberdeen, Cruickshank Building, St Machar Drive, Aberdeen, AB24 3UU, UK, tel. +44 (0)1224 273810, fax +44 (0)1224 272703, e-mail: pia.gottschalk@abdn.ac.uk

Abstract

When deforestation is followed by continuous arable cropping, a permanent decline of between 22 and 42% in the soil organic carbon (SOC) has been reported. This systematic loss of soil carbon (C) is mainly attributed to the loss of physically protected SOC. The Rothamsted Carbon model (RothC) does not include a description of the processes of physical protection of SOC and so losses of C during

continuous cultivation of previously uncultivated land are not likely to be accurately simulated. Our results show that in the first years following deforestation, RothC does not capture the fast drop in forest derived soil C. However, the model does satisfactorily simulate the changes in SOC derived from the following crops. Uncertainty in input data and accounting for erosion, does not explain the underestimation of decomposition after deforestation by RothC. A simple approach to increase decomposition by multiplying rate constants is evaluated. This approach needs high multiplication rates and leads to an overestimation of plant input values to sustain SOC equilibrium levels. However, the ability of RothC to simulate changes in the forest derived SOC can be greatly improved with an implementation of a simple approach to account for SOC dynamics due to the loss of physically protected C. This approach implements a new soil carbon pool into RothC which represents the labile but protected carbon fraction which builds up under minimally disturbed land uses, and which loses its protection once the soil is disturbed. The new pool is calibrated using ^{13}C natural abundance analysis in conjunction with soil fractionation.

Keywords: ^{13}C measurements, land use change, physical protection, Rothamsted carbon model, RothC, soil organic carbon modelling

1. Introduction

During the 1990s carbon dioxide (CO_2) emissions due to land use change are estimated to have been between 0.5–2.7 Pg C yr^{-1} out of the total emissions of 7.9 Pg C yr^{-1}, contributing 6–39% of the total emissions of CO_2 to the atmosphere (IPCC, 2007). Historically, emissions from land use change are estimated to have contributed 156 Pg C to the human induced CO_2 emissions occurring from 1850 to 2000 (Houghton, 2003), equivalent to 12–35 ppm (IPCC, 2007). Houghton (2003) estimated that 2.24 Pg C y^{-1} are attributable to the deforestation that occurred during the 1990s, thus being the biggest contributor to emissions in the land use change sector. Deforestation induces carbon (C) losses due to decay of vegetation and the decomposition of soil organic matter (SOM). Available assessments of historical soil C losses incorporate a high degree of uncertainty ranging from 40–537 Pg and so current net fluxes from the soil to the atmosphere are not well known at any national, regional or global scale (Lal, 2003). Therefore, a complete understanding of soil C fluxes, especially due to deforestation and subsequent continuous cultivation is of great importance in improving our estimates of C emissions from soils.

When forests and grasslands are converted to long term arable cropping, soil C is permanently lost to the atmosphere and the soil solution. A permanent decline of between 22 and 42% in the soil organic carbon (SOC) that was originally present under forest has been reported by Guo and Gifford (2002) and Murty et al. (2002). Soils lose most C in the first years following conversion (Houghton, 2003) until a new equilibrium level is established (Houghton, 1999; Guo and Gifford, 2002). This systematic loss of soil C across regions and site specific management is mainly attributed to the loss of physically protected SOC (Van Veen and Paul, 1981; Balesdent et al., 2000; Six et al., 2002). Physical protection of C occurs when organic

matter (OM) is trapped inside soil aggregates (Balesdent et al., 2000). This stabilisation effect occurs due to the physical segregation of substrate and micro-organisms, a reduced rate of oxygen diffusion into the aggregates and the separation of microbial biomass from microbial grazers (Six et al., 2002). This C pool is very sensitive to cultivation because the mechanical disturbance of the soil leads to a break up of aggregates which in turn releases C and makes is accessible to decomposition (Balesdent et al., 2000; Six et al., 2000; Denef et al., 2007). Here, we define the loss of soil aggregate structure and subsequent release of decomposable OM as the loss of physically protected SOC. Another important factor that can contribute to the decline in soil C is soil erosion (Balesdent et al., 2000). However, the absolute changes in soil C stocks and the temporal dynamics of the losses depend on management, climate and soil type for the particular site (Allen, 1985; Guo and Gifford, 2002; Schwendenmann and Pendall, 2006). To capture these complex and dynamic interactions, SOM models are employed. One of the most widely used models of soil C dynamics is the Rothamsted C model (RothC) (Coleman and Jenkinson, 1996). This model has been evaluated under a wide range of ecosystems, climate conditions (Coleman et al., 1997; Diels et al., 2004; Shirato et al., 2005; Kamoni et al., 2007) and land use change (Smith et al., 1997; Cerri et al., 2007). However, the model has not been widely evaluated against changes in SOC due to forest clearing followed by continuous arable cropping. Long term experiments previously used to evaluate the model, usually include long periods of the same or similar management practices, so do not show the C loss characteristic of forest clearing as assessed here. Because RothC includes neither an explicit description of the processes of physical protection of SOC or soil erosion, we postulated that losses of SOC during continuous cultivation of previously uncultivated land were not likely to be accurately simulated.

Only a few SOM models include an explicit description of physically protected SOC. Van Veen and Paul (1981) introduced two states, physically protected and not protected SOC into their model for long term SOC turnover. In that model, protected SOC has a relatively slower decomposition rate compared to its non-protected counterpart. The proportion of SOM that would be protected was indicated by a "protection coefficient" which was indirectly fitted to the simulation of SOC dynamics in virgin and cropped soils. In grassland soils, 50% of SOC was protected and under arable cropping, only 20% was protected. They hypothesised that the major factor of enhanced mineralization due to cultivation is the disruption of aggregates. Molina et al. (1983) used a resistant SOC pool, which is constantly formed and periodically transferred to a more labile pool during cultivation events. Hassink and Whitmore (1997) compared the performance of the RothC model to a model which they developed to explicitly describe the dynamics of protection and loss of protection of SOC. Their model is based on adsorption and desorption kinetics of SOM particles to clay surfaces and the rate at which SOM becomes protected depends on the fraction of the available protective capacity of a soil. The two models were applied to experimental soil treatments over 20 years. The model of Hassink and Whitmore (1997), which was calibrated at one of their sites, performed better for these trials, but described only 5% more of the variation in the data than RothC. Furthermore, the soils in their treatments were taken from arable fields and were regularly disturbed during the experiment, presumably being at or close to equilibrium in terms of soil aggregate structure. Their model of physical protection does not, therefore, describe the dynamics of physical protection and loss of physical protection due to land use or management change. We implement a simple approach to simulate the dynamics of physically protected C (within aggregates) due to land use change and the loss of soil

C due to erosion and compare, and discuss findings in relation to other models of physical protection.

SOM models are typically evaluated against measurements of total SOC. Relatively few studies have used $\delta^{13}C$ data to evaluate SOM models (e.g. Townsend et al., 1995; Balesdent, 1996; Molina et al., 2001; Diels et al., 2004; Niklaus and Falloon, 2006; Cerri et al., 2007). Measurements of $\delta^{13}C$ of SOC can be used to distinguish between C_3 and C_4 plant derived C. C_3 and C_4 plants discriminate differently between ^{12}C and the natural isotope ^{13}C. C_3 plants (most trees and herbs) develop a $\delta^{13}C$ signature that ranges from -23‰ to -40‰ whereas values for C_4 plants (some tropical grasses and cereals) range from -9‰ to -19‰ (Smith and Epstein, 1971). These distinct signatures are preserved during the decomposition of plant material in the soil. On soils where a complete shift from C_3 to C_4 plants has occurred, the difference in the isotopic signatures provides a means to infer the turnover time of SOM, distinguishing between the original SOM and the contribution of the succeeding vegetation (Balesdent and Mariotti, 1987). Linking ^{13}C abundance with SOM particle size fractionation techniques has been used by a number of different workers to assess quantitative changes of C in different soil size fractions (Balesdent and Mariotti, 1987; Balesdent et al., 1988, 1998; Vitorello et al., 1989; Martin et al., 1990; Desjardins et al., 1994; Jastrow et al., 1996; Paul et al., 2008; Schwendenmann and Pendall, 2006). However, there are only a few studies where model evaluation has used soil fractionation techniques (Skjemstad et al., 2004; Zimmermann and Leifeld, 2007) or the combination of ^{13}C abundance and soil fractionation techniques (Balesdent, 1996).

In our study we used total SOC data as well as $\delta^{13}C$ data from four chronosequence sites to evaluate the RothC model. The long term response of SOC to

147 forest clearance is not, therefore, represented by a single set of measurements from
148 long term sites but instead from measurements of plots with similar soil and
149 management characteristic but of different cropping ages. This introduces an inherent
150 inconsistency in the representation of climatic drivers used in the simulation. The
151 model simulates the C dynamics along a timeline defined by the sequence of climate
152 and management. Model results are then compared to the chronosequence
153 measurements as if they were taken in a long term trial (Smith et al., 2000). To
154 account for these inaccuracies, an uncertainty analysis was carried out to estimate the
155 variability in model results.

156 The objectives of this study are (i) to evaluate RothC at forest cultivation
157 sequence sites using ^{13}C abundance measurements, (ii) to assess the uncertainty of the
158 model results due to uncertainties in the input data, (iii) to use ^{13}C natural abundance
159 in conjunction with soil fractionation to evaluate the dynamics of the C pools of
160 RothC separately from total C dynamics, (iv) to account for soil erosion, and (v) to
161 implement a simple approach to simulate the dynamics of physically protected C.
162

163 **2. Materials and Methods**

164 2.1. Site description

165 The RothC model was run on four chronosequence sites, three in Zimbabwe,
166 Africa, and one in France, Europe. Climate, soils, vegetation and management of the
167 Zimbabwean and French sites and their C dynamics are described in detail in Zingore
168 et al. (2005) and Arrouays and Pelissier (1994) and Balesdent et al. (1998),
169 respectively. At the three Zimbabwean sites (hereafter referred to as Mafungautsi,
170 Masvingo and Chikwaka) miombo woodland was cleared for smallholder subsistence
171 farming cropping maize in monoculture. Miombo woodlands are mainly composed of

172 C_3 plants and maize is a C_4 plant. Therefore, the soils of the selected sites exhibit a
173 shift from C_3 to C_4 plant vegetation which enables the separation of soil C as
174 described in section 1. Inputs to the soils at all three Zimbabwean sites are minimal as
175 yields are very low (<100–300 g C m^{-2} $year^{-1}$) and maize stover is often used as cattle
176 feed, or it is burned. There is no use of mineral or organic fertilizer at the selected
177 sites. The soils at the three sites represent the major soil types under smallholder
178 farming in Zimbabwe and are situated in different climatic regions of the country. The
179 French chronosequence site is situated in the Pyrenean Piedmont, hereafter referred to
180 as the "Pyrenean" site. The soil at the Pyrenean site is a thick humic acid loamy soil.
181 Mature maritime pine forest (mainly C_3 plants) was cleared for intensive continuous
182 maize cropping with stalks returned to the soil, no organic fertilizer use and C returns
183 to the soil of about 500 g C m^{-2} $year^{-1}$. Table 1 gives an overview of the site
184 characteristics relevant for the model simulations.
185
186 2.2. The Rothamsted Carbon model
187 The Rothamsted C model (RothC) was originally developed for temperate
188 ecosystems (Smith et al., 2000), although model parameters encompass the
189 temperature sensitivity of SOM decomposition under tropical conditions as the model
190 was calibrated using data from Ibadan, Nigeria (Jenkinson, 1990).
191 The RothC model includes five pools of SOM: DPM (= decomposable plant
192 material), RPM (= resistant plant material), BIO (= microbial biomass), HUM (=
193 humified OM) and IOM (= inert OM). Each pool, apart from IOM, decomposes by
194 first order kinetics and using a rate constant specific to the pool. Each pool
195 decomposes into CO_2, BIO and HUM. The proportion of BIO to HUM is a fixed
196 parameter whereas the proportion of CO_2 to BIO+HUM varies according to the clay

content. Less clay leads to a relatively higher loss of CO_2. Decomposition is sensitive to the temperature, soil moisture and clay content of the soil, and so soil texture, monthly climate, land use and cultivation data are the inputs to the model (Coleman and Jenkinson, 1996; Smith et al., 1997). The model treats the effect of physical protection due to tillage implicitly by the DPM/RPM ratio of arable land use which was fitted to tilled arable soils (Jenskinson et al., 1991, 1992; Falloon, 2001). The model therefore accounts for the effect of regular disturbance on decomposition rates. The model also implicitly takes into account physical protection due to adsorption and desorption as the decomposition efficiency depends on the clay or CEC of the soil, leading to a greater protection of SOM in soils with a higher clay content. Decomposition in the RothC model is also sensitive to whether the soil is bare or not. Based on C^{14} labelled plant material decomposition measurements in bare and covered soils, Jenkinson introduced a plant retainment decomposition modifier in the model, which reduces decomposition rates by 40% in soils with actively growing vegetation. No reduction is assumed in soil where no vegetation is actively growing, or the soil is bare (Jenkinson et al., 1987). This empirical factor is not explicitly related to any physical or chemical decomposition parameters. It has been shown to work well (e.g. Coleman et al., 1997), which could be due to bare soils being more exposed to precipitation impacts, harsher drying-wetting cycles and higher soil temperature fluctuation. The effects are also indirectly caused by mechanical disturbance of the soil which again could be an indirect effect of physical protection (Balesdent et al., 2000).

2.3. Model input data

As site specific temperature, precipitation and open pan evaporation data were not available, monthly average temperature and precipitation data were retrieved from the CRU TS 2.1 global climate data set. This dataset is publicly available (http://www.cru.uea.ac.uk/) (Mitchell and Jones, 2005).

Monthly averages over a hundred year period (1901–2000) were calculated from the nearest grid values. Monthly potential evapotranspiration (ET_0) was calculated using the FAO Penman-Monteith approach (Allen et al., 1998) based on the CRU monthly temperature and vapour pressure. The values were then averaged over 100 years and multiplied by 1.33 to convert ET_0 derived from Penman-Monteith, into open pan evaporation values (Doorenbos et al., 1986; Coleman and Jenkinson, 1999).

Management schedules, soil texture and SOC for the African sites were taken from (Zingore et al., 2005) and Zingore (personal communication) (Table 1). Equivalent data for the Pyrenean site were taken from Balesdent et al. (1998) and Arrouays and Pelissier (1994) (Table 1).

Insert Table 1 here

2.4. Simulations

2.4.1. Default model application

The model was modified to distinguish between C derived from forest (C3 plants) and maize (C4 plants) and to compute soil $\delta^{13}C$ values of total organic C. Site simulations were run on constant yearly climate data and in two consecutive steps. First, the monthly soil inputs for maize were estimated, using the standard value of 1.44 for the DPM/RPM ratio. For the Mafungautsi site and the Pyrenean site,

246 estimates of C returned to the soil under arable conditions are given by the authors of
247 the original data, being 12 and 500 g C m^{-2} $year^{-1}$, respectively (Balesdent et al., 1998;
248 Zingore et al., 2005). For Masvingo and Chikwaka monthly soil inputs were
249 calculated by running the model to equilibrium using the total accumulated maize C,
250 which was assumed to have reached equilibrium. These values are 320 and 770 g C
251 m^{-2} as given by Zingore et al. (2005). In the second step, the model was run to
252 equilibrium for forest conditions (using the standard DPM/RPM ratio of 0.25)
253 followed by the period of maize cropping in the non-equilibrium phase of the
254 simulations. For the non-equilibrium phase of the simulation, the C inputs calculated
255 in the first step were used.
256 Since the model calculates soil C inputs from total soil C, these annual values
257 plus the amount of organic C removed from the site gives net primary production
258 (Jenkinson et al., 1999). Hence, the soil C input calculated from the forest equilibrium
259 site can be compared to NPP data for the forest. The values for the maize simulations
260 can be compared to the yearly SOM returns estimated from Zingore et al. (2005).
261
262 2.4.2. Adjusting IOM values for African sites
263 The measured $\delta^{13}C$ data of the forest derived C (Figs. 1 and 2 in Zingore et al.,
264 2005) show a steep decline in the first years of cultivation. After ca. 10–20 years the
265 decline levels off and C stocks do not change significantly. This suggests that the old
266 C is depleted in easily decomposable OM and has reached a level at which only very
267 recalcitrant C remains. Recalcitrant C is represented by the IOM pool in RothC. IOM
268 "represents a small, stable and biologically inert fraction of soil C, which has a high
269 radiocarbon age" (Falloon et al., 1998). It was originally determined from soil
270 radiocarbon data. Since these data are rare and expensive, Falloon et al. (1998)

developed a regression equation to estimate the size of the IOM pool from SOC. However, Falloon et al. (1998) conclude that "separate models of log(IOM) and log(SOC) content for each land use show significant relationships for all land uses except savannah". This suggests that the IOM equation might not be valid for dry miombo woodland which is a savannah ecosystem. The equations also have wide 95% confidence intervals (Falloon et al., 2000), reflecting the large variation around the regression line that is observed in the experimental data.

IOM is described chemically as a mixture of charcoal, geologically ancient coal and SOC trapped irreversibly in the soil (Falloon et al., 1998). Miombo woodlands are fire prone (Desanker et al., 1997) and it can be assumed that fire residues such as charcoal accumulate in the soil more than in many temperate ecosystems. We therefore adjusted the IOM pool in the simulations to a value close to the value given for the forest derived C stocks at the equilibrium reached under cultivation. These values were 860, 800 and 1460 g C m^{-2} for Mafungautsi, Masvingo and Chikwaka, respectively (Zingore et al., 2005). These adjustments are supported by recent findings of the relationship between measured charcoal and the IOM pool of RothC when it was applied to soils of two different regions in Australia. Analyses of 452 Australian soil profiles yielded poor correlation between SOC and black C (residue of incomplete combustion of biomass and fossil fuels). Furthermore, the Falloon et al. (1998) equation underestimated the average proportion of black C by 13.8%, where the average of the measured values was 20.4% and the estimated value was 6.6%. Default and adjusted IOM values in our study are 7.4, 8.2 and 9% and 44.1, 19, 44.9% for Mafungautsi, Masvingo and Chikwaka, respectively. Even the 44.1% and 44.9% are well within the ranges of the coefficient of variation of the measured mean black C content of the Australian soils. The authors suggest that the estimate

296 based on the Falloon et al. (1998) equation might not be applicable to ecosystems
297 where black C is a significant fraction of SOC.
298
299 2.4.3. Accounting for erosion
300 Erosion can account for significant soil C losses at a site. For the three
301 Zimbabwean sites, soil erosion is estimated as 1200 g soil m^{-2} $year^{-1}$ (Zingore et al.,
302 2005). Here we use a simple approach for estimating C losses based on the soil
303 erosion rate, SOC content (Van Oost et al.,2007) and a C enrichment factor (Kniesel,
304 1980). As total soil C decreases over time, the amount of C in 1200 g soil decreases as
305 well because the percentage C content per unit soil decreases over time. Furthermore,
306 the amount of C in the 1200 g soil m^{-2} that is eroded each year, follows the same first
307 order kinetic decline as total C. Total C decline is based on the C content in *x* g of soil
308 in 20 cm depth per hectare. The relative dynamic is the same as in 1200 g soil. Thus,
309 using the rate constants for a single exponential function estimated by Zingore et al.
310 (2005), we calculated the C lost each year. The percentage C loss amounted to ca.
311 0.4% of the total C per year for each site. The enrichment factor is calculated as
312 $7.4*(1000*\text{soil loss})^{-0.2}$ (Kniesel, 1980) and equates here to 1.13. We implemented
313 this simple approach in RothC by subtracting 0.4%*1.13 of the C from each pool each
314 year. At the Pyrenean site, no erosion is reported so no erosion term was used.
315
316 2.4.4. Accounting for "physically protected" C
317 At the Pyrenean chronosequence site Balesdent et al. (1998) studied the effect
318 of soil disturbance on SOC dynamics in several particle size fractions. They showed
319 that cultivation affects C dynamics in all particle size fractions. The fractions used by
320 Balesdent (1998) have been shown in other studies to correspond closely to the model

pools used in RothC (Balesdent, 1996; Skjemstad et al., 2004). Therefore, we used their data and findings to evaluate the C dynamics per model pool. The C contents of the different model pools were compared to C contents measured in the different particle size fractions: the C of the RPM pool was compared to the C of particle sizes >50 µm (particulate organic matter (POM)) and the sum of C in the DPM, BIO, HUM and IOM pool was compared to the C associated with particle sizes <50 µm.

Balesdent et al. (1998) show that SOC in the size fraction <50 µm is made up of the relatively rapidly decomposing pool of silt associated C, and a relatively slowly decomposing pool of clay associated C. The measured turnover of the clay associated C has a decay constant of 0.03 $year^{-1}$ (Balesdent et al., 1998). This value is close to the decay constant of the HUM pool of RothC (0.02 $year^{-1}$; Coleman and Jenkinson, 1999). Hence, these pools match closely in terms of decomposition dynamics. The silt associated C has a measured decay constant of 0.12 $year^{-1}$ but initially is also represented by the humus pool of the model. The Balesdent et al. (1998) analysis shows that the C in the silt size fraction declines almost as rapidly as that in the POM fraction. We hypothesized that we could represent the silt size fraction by an extra pool, giving it the decomposition rate of the HUM pool for the time under undisturbed land use and a decomposition rate similar to the RPM pool (0.3 $year^{-1}$) for the time under cultivation, to simulate the loss of physically protected C. We will refer to this extra pool as the “silt-humus” pool and the remaining HUM pool as the "clay-humus" pool. Each SOC pool of RothC would now decompose into BIO, silt-humus and clay-humus. The initial size of the silt pool was fitted to the amount of C in the silt size fraction under forest (RothC equilibrium run for forest conditions) by adjusting the proportions of C that decomposes into the silt-humus pool and the clay-humus pool. The sum of the two proportions equals the proportion that was previously flowing

346 only into HUM. The silt-humus pool would represent the labile fraction of the
347 protected SOC under undisturbed land use and would change to a non-protected SOC
348 pool under cultivation.

349 This concept is different from the concept of the model of physical protection
350 developed by Hassink and Whitmore (1997). In their model, total OM cycles between
351 a non-protected and protected SOM pool, where OM only decomposes in the non-
352 protected pool. The protected pool is therefore similar in concept to the IOM pool of
353 RothC, however in RothC IOM is not linked to the other active SOC pools. In the
354 model of Hassink and Whitmore (1997) the rate of protection depends on the amount
355 of free OM and the protective capacity of the soil. This parameter is linearly
356 correlated with the soil's clay content. The rate at which SOC loses its protection is
357 represented by a desorption rate constant. Both rate constants and the protective
358 capacity of the soil are indirectly fitted to soil C measurements of long term arable
359 soils. Therefore, their model parameters are only calibrated for arable soils with no
360 land use change.

361 Our concept is more similar to the model of Van Veen and Paul (1981) which
362 introduces SOM pools in two states: protected (e.g. under grassland) and not protected
363 (e.g. under cropping) and where OM decomposes slower in the protected pool. This
364 would relate to the new silt-humus pool in RothC, which is protected in non-disturbed
365 soils (here forest) and loses its protection in cultivated soils. Also, the decomposition
366 rate constant of the silt-humus pool decreases in non-disturbed soils.
367 The approach taken by Molina et al. (1983) is again different from our approach as in
368 their model, loss of physical protection is represented by an occasional transfer of C
369 from a resistant pool to a more labile pool at cultivation events.
370

2.5. Evaluation - Statistical analysis

Model results at all four chronosequence sites were evaluated against total organic C and against forest and maize derived C separately.

The model results were evaluated statistically using the approach proposed by Smith et al. (1996, 1997). The degree of association between simulated and measured values was determined using the correlation coefficient (*R*), and the significance of the correlation was assessed using a Student's *t* test. This tells us whether the two sets of data have the same trend, and is important if the results are to be extrapolated beyond the scope of the experiment. Values for *R* range from -1 to +1. Values close to -1 indicate a negative correlation between simulations and measurements, Values of 0 indicate no correlation and values close to +1 indicate a positive correlation (Smith et al., 1996; Smith and Smith, 2007).

The coincidence between the measured and simulated values was assessed by calculating the root mean squared deviation (*RMS*) (Smith et al., 2002; Smith and Smith, 2007). This is the average total difference between measured and simulated values and is given in the same units as the analysed data. The lower the value of *RMS*, the more accurate the simulation.

The bias in the simulations with respect to the measurements was calculated as the mean difference (*M*) (Addiscott and Whitmore, 1987). *M* does not include a square term, so simulated values above and below the measurements cancel each other out. Therefore, inconsistent errors will not be considered and values of *M* will be either positive or negative if the simulation results are biased. *M* will be zero if there is no difference between simulated and measured values. The significance of *M* can be tested using a Student's *t* test (Smith et al., 1996, 1997; Smith and Smith, 2007).

396

397 2.6. Uncertainty analysis

398 Using chronosequence data as a surrogate for long term experimental data in
399 model evaluation is inherently uncertain as space is used to substitute for time.
400 Samples are taken from different plots, reflecting different points in time after a land
401 use or management change, instead of taking samples from the same plot over time.
402 In addition, inaccuracies are introduced in the simulations because the simulations
403 must be based on average climate data rather than a continuously varying climate. To
404 account for these uncertainties in the model evaluation, the response of the model
405 towards possible variations in input data was assessed by an uncertainty analysis.

406 The uncertainty analysis followed a Monte Carlo approach. Ranges of input
407 data were defined and sampled 500 times using Latin Hypercube Sampling. RothC
408 was run on the 500 samples, each run using a different combination of input data. This
409 approach was chosen to encompass the interaction of input data in the model results.
410 The uncertainty ranges of the driving variables temperature, precipitation and clay
411 content were set according to information from the literature and electronic databases.
412 All ranges were assumed to be uniformly distributed.

413 Climate uncertainty ranges for the sites in Zimbabwe were based on minimum
414 and maximum yearly values given by (1) CRU 100 year and 30 year (1961–1990)
415 average, (2) MarkSim weather generator (Jones and Thornton, 2000) and (3) data
416 from the Zimbabwe Meteorologic Service Department (ZMSD) (supplied by S.
417 Zingore, personal communication) (Table 2). For the Pyrenean site, only CRU 100
418 year average data were available. To generate uncertainty ranges, we used the average
419 relative ranges of the Zimbabwean sites.

420

421 Insert Table 2 here

422

423 Uncertainty ranges for clay were based on minimum and maximum values
424 given in the FAO data base for given soil types (Batjes, 2002). Only the soil types of
425 the African sites are present in that data base. Measured standard deviations of the
426 clay content by Balesdent et al. (1998) are comparably small, so we interpolated the
427 minimum and maximum values given for the African sites to the Pyrenean site so as
428 to obtain comparable ranges. Ranges are given in Table 2.

429

430 **3. Results and discussion**

431 3.1. Plant input estimation

432 Plant input for maize simulations at Masvingo and Chikwaka were estimated
433 by the model to be 36 and 63 g C m^{-2} $year^{-1}$, respectively, and 11 g C m^{-2} $year^{-1}$ for
434 Mafungautsi when run in the same mode. SOC under maize at the Pyrenean site had
435 not reached equilibrium (Arrouays and Pelissier, 1994) so could not be used to
436 calculate plant input values by running the model to equilibrium.

437 Maize plant input values for Masvingo and Chikwaka can only be compared
438 relative to the estimate given by Zingore et al. (2005) for the Mafungautsi site, which
439 is 12 g C m^{-2} $year^{-1}$. Similarly derived estimates for Masvingo and Chikwaka are
440 highly uncertain, as stated by Zingore et al. (2005). The deviation in the values
441 simulated at Masvingo and Chikwaka from the measurements at Mafungautsi can be
442 explained by considering the differences in the sites. Masvingo has a higher clay
443 content and supports higher average yields than Mafungautsi (Zingore et al., 2005). It
444 can be assumed that the finer textured soil has a better moisture regime and inherent
445 soil fertility which results in the higher observed crop yields, and therefore higher C

446 returns to the soil. These higher soil inputs sustain the observed higher C stock.
447 Average decomposition rates are presumably slower in the clay soil than in the sandy
448 soil and simulated C returns should be lower in the clay soil than in the sand soil.
449 However, that would only be true if the C stocks in the two different soils are similar.
450 The total difference of maize C stock in the Mafungautsi soil and the Masvingo soil is
451 240 g C ha^{-1}, being 80 g C ha^{-1} and 320 g C $ha^{-1}$for Mafungautsi and Masvingo,
452 respectively. Similarly, at Chikwaka, where the clay and C contents (770 g C ha^{-1}) are
453 even higher than at Masvingo, the simulated C returns are higher, which again
454 correlates with even higher average yields as Chikwaka than at Masvingo. Confidence
455 in these values is increased by the good fit between the maize derived C simulations
456 and the measured values (see section 3.2. and Table 3). It can therefore be assumed
457 that the simulated higher returns for the finer textured soil are due to the higher C
458 stock, and these are only partly balanced by a slower average turnover.
459 Plant input values for the equilibrium run under forest were 179, 184, 248 and
460 898 g C m^{-2} $year^{-1}$ for Mafungautsi, Masvingo, Chikwaka and the Pyrenean sites,
461 respectively. However, there are no measurements of NPP for comparison with
462 simulated plant input values for forest. We therefore compare our simulated values for
463 the African sites to data published in related literature. Frost (1996) estimates net
464 biomass production between 120 and 200 g m^{-2} $year^{-1}$ for dry miombo woodlands,
465 corresponding to 54 and 90 g C m^{-2} $year^{-1}$. Brown et al. (1994) gives an estimate of
466 368 g C m^{-2} $year^{-1}$, as a combined value of above and below ground input to a dry
467 miombo woodland site in Zimbabwe. Similarly, Jenkinson et al. (1999) simulated a
468 plant input of 374 g C m^{-2} $year^{-1}$ for a natural woodland site in Zambia, on a Haplic
469 Ferrasol, with an annual rainfall of 1245 mm within a single wet season, November to
470 April. The values estimated by the model (179, 184, 248 g C m^{-2} $year^{-1}$) lie well

471 within the published ranges of estimated plant inputs of miombo woodlands (54 to
472 374 g C m^{-2} $year^{-1}$).

473 For the Pyrenean site estimates for forest above ground plant inputs are given
474 by Balesdent et al. (1998) to be 150–250 g C m^{-2} $year^{-1}$ as leaves, fruit and small
475 branches. These values refer to measurements at forest stands in the same region. In
476 forests, fine root turnover can be estimated to be approximately the same amount as
477 litter fall (Zianis et al., 2005), which would amount to ca. 300–500 g C m^{-2} $year^{-1}$ of
478 total plant inputs. The MODIS satellite derived NPP values (Running et al., 2004) for
479 forest stands in the same region were extracted and range between 510–810 g C m^{-2}
480 $year^{-1}$ for the three sites in 2000 and 2002. At 898 g C m^{-2} $year^{-1}$, the model estimates
481 of plant inputs under forests at the Pyrenean site are slightly higher than these
482 measurements (150–810 g C m^{-2} $year^{-1}$).
483

484 3.2. Carbon dynamics of simulations without adjustment of IOM for the specific site,
485 simulation of erosion or physical protection

486 The results of simulations not including erosion or physical protection suggest
487 that RothC does not capture the soil C response after forest clearing for continuous
488 cropping, neither in the tropics nor in the temperate ecosystem.

489 The default model simulations for the sites in Zimbabwe of total C dynamics
490 (Fig. 1) show that the rapid loss of soil C in the first years of cultivation is not
491 captured by the model and that the continuous C loss towards the end of the
492 simulation is overestimated and does not reach a plateau as can be seen in the
493 measured data (Figs.1 and 2 in Zingore et al., 2005). Simulated forest derived C
494 would eventually level off at the level of IOM, as it does not receive any new plant
495 inputs.

Insert Figure 1 here

This was a surprising result as RothC has been shown to simulate deforestation well in the Brazilian Amazon region (Cerri et al., 2007). However, these sites were converted to well managed pastures and do not exhibit a substantial C loss. Diels et al. (2004) applied RothC in a sub-humid tropical climate. Their results show that RothC also underestimates C losses compared to measured values. However, several years of grassland precede the simulated cropping experiments and we hypothesise that the same explanation holds for the findings of Diels et al. (2004) as for the experiments studied here. Under undisturbed grassland, the SOC became physically protected and accumulated in a labile, though protected, C pool. This C decreased rapidly once the cropping experiments started, and RothC did not capture this dynamic. Similar modelling results were shown by Coleman et al. (1997) when the RothC model was applied to the Highfield bare fallow experiment in Rothamsted, England. That site was grazed grassland for several hundred years until it was ploughed and converted to bare fallow. RothC underestimated C loss after the conversion. Moreover, the plant retainment factor was set to 1.0 in these simulations, compared to the set up in our study where only half of the year was assumed to exhibit bare soil conditions. Therefore, decomposition was even relatively faster in the simulations of Coleman et al. (1997) than in our study. Again, the same explanations as given for the study of Diels et al. (2004) hold for the Highfield bare fallow experiment. Note that an earlier version of RothC also underestimated C losses when old grassland was ploughed (Jenkinson et al., 1987).

521 Insert Figure 2 here

522

523 Figure 2 shows a higher contrast picture of the measured and simulated C
524 changes, distinguishing between forest and maize derived C dynamics. The
525 simulations of the forest derived C show the same pattern as observed in the
526 simulation of total C. However, simulated C accumulation shows a good fit to the
527 measured maize C (Table 3).

528

529 Table 3 here

530

531 At Mafungautsi, Chikwaka and Pyrenean, *R* values show a significant ($p < 0.05$)
532 association between simulated and measured values. However, at Masvingo the
533 association is not significant. Zingore et al. (2005) state that $\delta^{13}C$ values at Masvingo
534 increase rapidly in the first years, but are not sustained because of the small returns of
535 maize residues and the low capacity of the soil to stabilize C. It is likely that maize
536 yields were somewhat higher in the first years and decreased after time of cultivation.
537 This might explain the higher than simulated observations of $\delta^{13}C$ at the beginning of
538 cultivation. In our simulations, we did not consider changing yields since there were
539 no reliable estimates of the impact of changing yield on residue returns. Residue
540 returns were based on RothC equilibrium runs using measured equilibrium soil C
541 stocks. These stocks do not reflect the variability in the first years of cultivation.
542 However, a better fit could be achieved by adjusting the inputs for the first years of
543 the simulation.

544 The *RMS* values can be compared directly between simulations, but since no
545 standard errors were available for the $\delta^{13}C$ values, the statistical significance of *RMS*

546 could not be assessed. The simulation of the Pyrenean site shows the least coincidence
547 with the highest value of *RMS* of 610 g C m^{-2}, compared to 204 for Chikwaka, 202 for
548 Masvingo and 21 g C m^{-2} for Mafungautsi.

549 The calculated values of *M* indicate that the simulation at Mafungautsi shows
550 the lowest bias, with a slight, consistent overestimation of 15 g C m^{-2}. At Masvingo
551 and Chikwaka, the model systematically underestimates soil C by 127 and 123 g C
552 m^{-2} respectively. The highest bias is observed in the simulated values at the Pyrenean
553 site, where the model overestimates soil C by 441 g C m^{-2}. However, the bias is only
554 statistically significant at Masvingo ($p < 0.05$).

555 These results suggest that the lack of fit between the simulations and the
556 measurements can mainly be attributed to the simulated underestimation of forest C
557 loss, and not to the simulation of maize C. This supports the hypothesis that there is a
558 need to account for the accumulation of physically protected SOM under uncultivated
559 land uses and to simulate the loss of physical protection due to cultivation.

560 Diels et al. (2004) found that doubling the decomposition rates of RothC to
561 account for a faster loss of SOC gave a better fit to their observed data. However, a
562 general increase of decomposition rates would also lead to higher plant input values in
563 the forest equilibrium runs. For illustrative purposes we tested for the Mafungautsi
564 and the Pyrenean site, how much change in the decomposition rates was necessary to
565 achieve a good fit to the observed data. For the Mafungautsi site, decomposition rates
566 of all pools needed to be multiplied by 10 to achieve a significant association for the
567 forest derived C. SOC accumulation under maize which was previously slightly
568 overestimated by 15 g C m^{-2} was now slightly underestimated by 5 g C m^{-2}. However,
569 there was no significant association between the simulation and the measurements
570 anymore as in the default model application. Furthermore, simulated plant input

values for forest increased to the unrealistic value of 1010 as compared to 179 g C m^{-2} $year^{-1}$ of the default simulations and published values of between 54 and 374 g C m^{-2} $year^{-1}$. At the Pyrenean site, decomposition rates were multiplied with four to get a good association (R value of 0.99) for the forest derived C, however it was not significant. The R value for the maize derived C still shows a significant association and the coincidence improved slightly to and *RMS* of 568 g C m^{-2} but simulated values are now underestimated by 440 g C m^{-2}. Furthermore, plant input values for forest increased to an unrealistic value of 3570 compared to 898 g C m^{-2} $year^{-1}$ in the default simulations and MODIS derived NPP ranges of 510–810 g C m^{-2} $year^{-1}$. Again, these results suggest, that the model needs to take into account the dynamics of physical protection and loss of physically protected SOC due to land use and land use change. A simple increase of turnover rates does not present a valid and consistent solution.

3.3. Carbon dynamics of simulations including correction for the IOM content at the given site

When the adjustment of IOM is included in the simulations, the model no longer overestimates C loss towards the end of the simulations (Figure 3). The C changes appear to level off close to measured values once the model captures the rapid C loss at the beginning of the simulations.

Insert Figure 3 here

Simulations with the higher IOM values also results in a change in the forest plant inputs simulated at equilibrium. These have decreased from 179, 184, 248 g C

596 m^{-2} $year^{-1}$ to 108, 129 and 176 g C m^{-2} $year^{-1}$ for Mafungautsi, Masvingo and
597 Chikwaka, respectively. These values still lie within the range of published plant
598 inputs of 54–374 g C m^{-2} $year^{-1}$.

599 RothC estimates of steady state plant input are linearly correlated with the
600 total active C stock. A larger active C pool leads to a higher plant input requirement
601 than a smaller active pool, compared under the same environmental conditions. Thus,
602 since the IOM pool was adjusted to a higher value, the "active" C pool decreases and
603 simulated inputs became smaller as well.

604 These results show that the default equation for IOM given by Falloon et al.
605 (1998) is not valid for the simulation of savannah ecosystems here. Falloon et al.
606 (1998) noted that this equation might not be valid for savannah ecosystems. However,
607 the values we used for our simulations lie within the 95% confidence interval of the
608 Falloon (1998) equation (Table 4).

609

610 Insert Table 4 here

611

612 In contrast, at the French site the simulation curve levels off towards the end
613 of the simulation. The stable SOC is estimated by Balesdent et al. (1998) to be about
614 2300 g C m^{-2}. This relates to the IOM pool in the model, which is estimated by the
615 Falloon (1998) equation to be 2302 g C m^{-2}. Again, the C changes appear to level off
616 close to measured values once the model captures the rapid C loss at the beginning of
617 the simulations.

618 The IOM adjustment does not affect the simulations of soil C accumulation
619 under maize because the IOM pool in RothC is not integrated in the decomposition

dynamic itself, but acts as a separate, inert pool that accounts for high radiocarbon ages of soils (Jenkinson et al., 1987). It is zero for the maize derived C.

3.4. Carbon dynamics of simulations including C loss by erosion

For illustrative puposes, we show the simulations for only the Mafungautsi site (Fig. 4), where the IOM is adjusted and C loss by erosion is simulated. The C loss from erosion was too small to explain the high rates of decline of forest derived soil C observed in the measurements. Erosion has only a small effect on the total soil C under maize. *R*, *RMSE* and *M* values are 0.69, 20 g C m^{-2} and -14 g C m^{-2} compared to 0.69, 21 g C m^{-2} and -15 g C m^{-2} for the default simulation, respectively. Diels et al. (2004) also suggested that a possible explanation for the discrepancy they observed between simulations and measurements was the additional losses of C due to erosion. However, even with erosion losses greater than 1200 g C m^{-2} $year^{-1}$, they concluded that these losses were negligible compared to the C loss due to decomposition.

Insert Figure 4 here

3.5. Implementation of a simple approach to describe physical protection of soil C

Figure 5 shows the simulation of total soil C and the soil contained in the DPM, BIO, HUM and IOM pool. The difference between the two curves represents the C contained in the RPM pool. The measured total soil C and measured soil C within particle size fraction <50 µm, respectively are shown as points on the plot.

Insert Figure 5 here

The graph on the left hand side shows the simulations of the forest derived C. The initial fast decline can be attributed to the loss of C from the RPM pool. The initialization of the RPM pool shows close agreement to the measured C in the >50 µm, whereas the sum of the pools DPM+BIO+HUM+IOM shows close agreement with the measured C in the <50 µm fraction. The RPM pool shows a similar decline in the first years to that observed in the C in the particle size fraction >50 µm. After the C in the RPM pool is depleted, the continued decline in soil C is dominated by the dynamics of the HUM pool. This is because the DPM and BIO pools contain a very small proportion of the total soil C. These remaining pools are the main cause of the underestimation of C loss as the decline of the RPM pool closely matches the decline in the soil C in the size fraction >50 µm. The results of the maize simulation (graph on the right hand site of Fig. 5) show a good agreement between the simulation and the measurements seven years after the start of the simulation. After 35 years, both curves exceed the measurements. After 35 years, the overestimation can be mainly attributed the accumulation of C in the humus pool. The accumulation in the RPM pool again shows close agreement with the amount of C in the measured POM fraction. Maize inputs for the Pyrenean site were 500 g C m^{-2} $year^{-1}$. This value was derived from measured above ground input of 350 g C m^{-2} $year^{-1}$ (stems and leaves) and below ground inputs of 150 g C m^{-2} $year^{-1}$ (roots) (Balesdent at al., 1998). To give a better fit to the maize C measurements of the Pyrenean site, plant inputs need to be decreased to 350 g C m^{-2} $year^{-1}$ (-30%). However, that does not result in an improvement of the total C simulation. Balesdent (1996) found that he had to decrease soil inputs simulated with RothC at a similar site by 17% compared to the measured values to match the measured data for maize accumulation.

669 For simulation of both forest and maize derived soil C, the results suggest that
670 the slow turnover of the HUM pool is the main cause of the discrepancy between the
671 simulation and the measurements. Simulated forest C does not decompose quickly
672 enough, resulting in an underestimation of soil C loss. The maize derived soil C is
673 simulated to accumulate more rapidly in the humus pool than the measurements
674 would suggest, which again is the result of the simulated turnover of the humus pool
675 being too slow. It has been shown that changes to turnover rates of the RothC pools
676 may account for processes which have previously not been included in the model
677 (Falloon et al., 2006). However, none of these studies address processes related to the
678 physical protection of SOC in soil.
679 Figure 6 shows the simulated values at the Pyrenean site after the
680 implementation of the extra humus pool. In the original RothC model, the C flux is
681 divided between the BIO and HUM compartment in proportions 46% and 54%,
682 respectively. Fitting the model to set the silt-humus pool from the initial measurement
683 of silt associated C, results in the C flux being divided into the BIO, silt-humus and
684 clay-humus pools in proportions 46, 39 and 15%, respectively (Fig. 7). Table 5 gives
685 the results of the statistical evaluation to compare the simulations and measurements
686 of forest and maize derived C. Note that only the test results for the maize derived C
687 are an independent test, because the first measurement of silt associated forest C was
688 used to fit the new ratio of the C fluxes into BIO, silt-humus, and clay-humus pools.
689 All correlation coefficients for the simulation of the maize derived C are 0.99,
690 indicating a very high association between the simulation and the measurements.
691 However, since only three measurements were available for the evaluation, the
692 statistical values are not significant ($p > 0.05$). The error in the simulation of total soil
693 C is decreased from 610 g C m^{-2} for the default simulations to 147 g C m^{-2} for the

694 results including the silt-humus pool. The bias of total soil C has also decreased from
695 -441 of the default simulation down to -110 g C m^{-2}. The slight overestimation of 110
696 g C m^{-2} is not significant ($p > 0.05$).
697
698 Insert Figure 6 here
699
700 Insert Table 5 here
701
702 Insert Figure 7 here
703
704 These results show that the implementation of the silt-humus pool into RothC
705 improved the simulations, but since measurements of only three points in time were
706 available to evaluate the results, we cannot show the improvement in statistical
707 significance. Balesdent et al. (2000) had already suggested that most of the protected
708 SOM occurs in the slowly decomposing pool of small sized SOM found in
709 microaggreagates, referring explicitly to the humus pool of the RothC model. An
710 early version of RothC included two humus pools, one representing physically
711 stabilized OM and one representing chemically stabilized OM (Jenkinson and Rayner,
712 1977). However, this concept was dropped and the protective effect of soil texture on
713 decomposition dynamics was implemented by adjusting the ratio of
714 CO_2/(BIO+HUMUS) based on the cation exchange capacity of a soil. The proportions
715 were based on experiments of Sorensen (1975) who studied the decomposition of ^{14}C
716 labeled plant material in soils of different textures. This effect does, therefore, account
717 for the process of the natural binding and entrapment of OM to and within mineral

718 material. It does not, however, account for the mechanical disturbance of soil and
719 consequent effect on OM decomposition.
720
721 3.6. Uncertainty analysis
722 Results show that the general trends in the simulations are not altered by
723 varying inputs within the range of the uncertainty. Uncertainty ranges are different for
724 each site. Yearly average temperature and yearly sums of precipitation ranges varied
725 between 0.67 and 1.51 ºC and 8–36% respectively. These ranges are similar to
726 interpolation errors estimated for a 10" climate data set of Europe. These are 13–20%
727 for precipitation and 0.8–1.1˚C for temperature (New et al., 2002). We used 100 year
728 average data to drive the simulations; it is possible that actual meteorological data,
729 showing inter-annual variability, would have increased output uncertainty to a degree.
730 Yearly sums of precipitation data do not show any significant trend ($p>0.05$), whereas
731 yearly mean temperature data show a significant trend ($p<0.05$) at Masvingo,
732 Chikwaka and Pyrenean of +0.8, +0.7 and +1.2 ºC. Likewise, PET values show a
733 significant trend ($p<0.05$) of +60, +45 and +50 mm $year^{-1}$, respectively. The effect on
734 decomposition of these two significant trends would counteract each other as higher
735 temperatures increase decomposition and higher PET values dry out the soil more and
736 would decrease decomposition. Therefore, the trend would probably not be reflected
737 in a higher decomposition of SOM. Furthermore, simulations and the course of SOM
738 of chronoseqeunces cannot account for the site specific climatic changes because sites
739 are not simulated over the course of time but along sites of different ages of which the
740 measurements of the “youngest” sites (here: forest) constitute the “oldest” (initial) in
741 terms of simulation dates. A simulation of a long term experiment with given climatic
742 trends could certainly not be accurately simulated with average climate data as the

743 forest sites would have developed under a “cooler” climate than the arable sites.
744 However, these climatic effects are not reflected in chronosequence data. Inter annual
745 climatic variability is naturally high at the study sites, however, the effect of year to
746 year fluctuations on SOM would be small. Figure 8 shows the spread of the
747 simulation curves resulting from the uncertainty analysis. Results are similar at all
748 four sites. The variability in the simulation curves is very small and the spread
749 increases with time. Outputs of the Monte Carlo results are normally distributed at all
750 sites (Kolmogorov-Smirnov, $p>0.05$) apart from at Mafungautsi which is negatively
751 skewed. However, the distribution does not significantly deviate from a normal
752 distribution ($p>0.05$). The variability in the plant input values of the equilibrium runs
753 are small. They lie around -10 to -17% and +12 to 22% for forest and -12 to -14% and
754 +14 to 17% for maize (Table 6). Values are normally distributed at Chikwaka for
755 forest and maize and at Pyrenean for forest. Values at Mafungautsi and Masvingo are
756 positively skewed ($p<0.05$) for forest and maize, respectively. The positive skew
757 means that the peak of the plant input distribution is shifted towards lower values
758 compared to a normal distribution. Lower plant input values are due to the simulation
759 of a slower turnover. This might be a non linear response of the soil moisture
760 decomposition modifier at very low clay values as the soil dries out quicker from a
761 certain threshold onwards. However, this has a negligible effect on the simulation of
762 the C dynamics afterwards and average plant input values are close to the values used
763 in the default simulations. A small overall response of the RothC model towards
764 climate and clay input data has also been shown by Janik et al. (2002). This shows
765 that the results of our default simulations lie well within the range of possible results
766 when taking input data uncertainty into account. The reason why the default
767 simulation at Chikwaka runs along the outer limit of the uncertainty results is that the

768 climate data used for the default simulation represent a slightly warmer and drier
769 climate than the average of the climate data used for the uncertainty analysis.

770

771 Insert Figure 8 here

772

773 Insert Table 6 here

774

775 Although the range of results due to the uncertainty in the inputs is initially
776 small, the uncertainty in the results has a cumulative effect as the simulations
777 continue. The effect of an input data set which reflects rather unfavourable conditions
778 for decomposition, e.g. cold and dry, accumulates over the years. This sets the
779 extreme boundaries for the simulation curve, and the true value lies within the
780 minimum and maximum result. From the uncertainty analysis we can conclude that
781 the uncertainty of the input data does not explain the discrepancy between model
782 results and measured data, and that the model is not very sensitive to the uncertainty
783 ranges that are relevant for the given situations.

784

785 **4. Conclusions**

786 While RothC can satisfactorily predict the accumulation of maize derived C,
787 the simulations do not capture the fast decrease in forest C that occurs during the first
788 years of cultivation. However, when the forest and arable soils are at steady state, the
789 calculated input of plant C to the soil compare well with plant input values obtained
790 from estimates of NPP. This suggests that the model provides good estimates of plant
791 inputs.

792 If land use change has occurred from a uncultivated (forestry, grassland or
793 natural) to cropped in the last 30 years, the model in its current form may not be
794 reliable. If land use change has occurred before this time, we can assume that most of
795 the physically protected soil C has been released into unprotected pools, and the
796 model will provide more accurate simulations.

797 The new pool does not change previous RothC application results as it would
798 be rather small under arable cropping, however, it will have a significant effect on
799 simulations of changes from uncultivated land to cultivated and vice versa.

800 Having excluded other explanations for the underestimation of forest derived
801 C losses simulated by the model, our results suggest that the physical process of
802 disturbing the stable forest soil structure could be the source of the increased rate of
803 decomposition. We hypothesise that this is the main explanation for the rapid C loss
804 observed at the chronoseqeunce sites included in our study. The implementation of a
805 simple approach to account for the loss of physically protected soil C has given good
806 first results. However, this new approach needs further evaluation, especially to test
807 its performance on the simulation of tillage and no-tillage as this will reveal its
808 general applicability to simulate the dynamics of the physical protection of C.

809 It has also been shown that simply increasing decomposition by multiplying
810 the turnover rates of the model pools does not present a valid solution to simulate the
811 fast loss of forest derived C under cultivation. Simulated plant input values for the
812 equilibrium phase under forest become unrealistically high and the accumulation of
813 maize derived C becomes underestimated.

814 Our simple approach to simulate the loss of physically protected C due to the
815 cultivation of soil is similar to the model of physical protection of Van Veen and Paul
816 (1981). They introduced SOM pools in two states: physically protected and not

physically protected (with a reduced life time). This separation was based on a study of the protective effect of the soil matrix on the decomposition of amino acids. At that time, no experimental data were available to quantify the effect of disruption of soil by cultivation on mineralisation. Our approach now provides means to quantify the effect of physical protection and loss of physical protection on SOM decomposition.

A comparison between RothC and the model of physical protection of Hassink and Whitmore (1997) had shown that both models perform similar at soils under arable conditions (Hassink and Whitmore, 1997). The model of Hassink and Whitmore (1997) is based on the adsorption and desorption kinetics of SOM particles to clay surfaces which is also implicitly included in the RothC model. However, these dynamics do not explain the loss of C due to the disruption of soil aggregates.

Our results are in good agreement with recent studies on SOM dynamics that have focused on the biological and physiochemical processes and control of SOM stabilisation and turnover. Instead of using definitions based on chemical fractionation techniques research has moved on to assessing the location of OM in the soil structure using physical fractionation methods (Koegel-Knabner, 2006). It has been proposed by several authors that SOM turnover might be dominated by the location of SOM in the soil aggregates rather than its chemical recalcitrance (Van Veen and Paul, 1981; Balesdent, 1996; Six et al., 2000).

Our simple approach agrees with the conceptual model of soil C stabilisation developed by Six et al. (2002). He proposes that SOM turnover can be divided into three general pools: an unprotected pool which would be represented by the RPM pool, a physically protected pool which would be represented by the silt-humus pool and a bio-chemically protected soil C pool which would be represented by the clay-humus and IOM pool. However, the quantitative description and parameterisation of

842 such a model would be far too data extensive for the current application. The major
843 advantage of our simple approach is that it does not require any more data input than
844 the current model and would not compromise its regional, national and global
845 applicability.

846 In addition, our study has shown that the combination of ^{13}C abundance with
847 SOM particle-size fractionation techniques is an excellent tool for evaluating the
848 performance of a SOM model under land use change conditions. It allowed the
849 structural reasons for the model not providing good simulations of soil C changes
850 after these land use change to be identified. It also provided a valuable tool for
851 developing and testing a new implementation of physically protected C.

852 Our approach makes model pools measurable. This is a major step forward in
853 the evaluation of the different, and up to now, conceptual model pools.

854

855 **Acknowledgements**

856

857 We thank Manuel Martin, Stéphanie Jalabert and Dominique Arrouays for their help
858 classifying the soil type at the French chronosequence site in the FAO soil type
859 classification framework. We thank the European Union for funding this research
860 through the AfricaNUANCES Project (contract no. INCO-CT-2004-003729). We also
861 like to thank the reviewers of the first draft for their constructive comments.

862

863 **References**

864 Allen, J.C., 1985. Soil response to forest clearing in the United States and the tropics:
865 Geological and biological factors. Biotropica 17(1), 15-27.

866 Allen, R.G., Pereira, L.S., Raes, D., Smith, M., 1998. Crop evapotranspiration -
867 Guidelines for computing crop water requirements. FAO Irrigation and
868 drainage paper 56, FAO, Rome.
869 Arrouays, D., Pelissier, P., 1994. Changes in carbon storage in temperate humic
870 loamy soils after forest clearing and continuous corn cropping in France. Plant
871 and Soil 160(2), 215-223.
872 Balesdent, J., 1996. The significance of organic separates to carbon dynamics and its
873 modelling in some cultivated soils. European Journal of Soil Science 47(4),
874 485-493.
875 Balesdent, J., Besnard, E., Arrouays, D., Chenu, C., 1998. The dynamics of carbon in
876 particle-size fractions of soil in a forest-cultivation sequence. Plant and Soil
877 201, 49-57.
878 Balesdent, J., Chenu, C., Balabane, M., 2000. Relationship of soil organic matter
879 dynamics to physical protection and tillage. Soil and Tillage Research 53(3-4),
880 215-230.
881 Balesdent, J., Mariotti, A., 1987. Natural ^{13}C abundance as a tracer for studies of soil
882 organic matter dynamics. Soil Biology and Biochemistry 19(1), 25-30.
883 Balesdent, J., Wagner, G.H., Mariotti, A., 1988. Soil organic matter in long-term field
884 experiments as revealed by carbon-13 natural abundance. Soil Science Society
885 of American Journal 52, 118-124.
886 Batjes, N.H., 2002. Soil parameter estimates for the soil types of the world for use in
887 global and reginal modelling (Version 2.1; July 2002). ISRIC Report 2002/02c
888 [Available on-line at http://www.isric.org]. International Food Policy Research
889 Institue (IFPRI) and International Soil Reference and Information Centre
890 (ISTRIC), Wageningen.

891 Brown, S., Anderson, J.M., Woomer, P.L., Swift, M.J., Barrios, E., 1994. Soil
892 biological processes in tropical ecosystems. In: Woomer, P.L., Swift, M.J.
893 (Eds.), The biological management of tropical soil fertility. John Wiley,
894 Chichester, 15-46
895 Cerri, C.E.P., Easter, M., Paustian, K., Killian, K., Coleman, K., Bernoux, M.,
896 Falloon, P., Powlson, D.S., Batjes, N., Milne, E., Cerri, C.C., 2007. Simulating
897 SOC changes in 11 land use change chronosequences from the Brazilian
898 Amazon with RothC and Century models. Agriculture, Ecosystems and
899 Environment 122(1), 46-57.
900 Coleman, K., Jenkinson, D.S., 1999. RothC-26.3: A model for the turnover of carbon
901 in soil - Model description and Windows user guide. IACR-Rothamsted.
902 Coleman, K., Jenkinson, D.S., Crocker, G.J., Grace, P.R., Klir, J., Korschens, M.,
903 Poulton, P.R., Richter, D.D., 1997. Simulating trends in soil organic carbon in
904 long-term experiments using RothC-26.3. Geoderma 81(1-2), 29-44.
905 Coleman, K.W., Jenkinson, D.S., 1996. RothC-26.3 - A model for the turnover of
906 carbon in soil. In: Powlson, D.S., Smith, P., Smith, J. (Eds.), Evaluation of soil
907 organic matter models using existing long-term datasets, 38, NATO ASI
908 Series I. Springer-Verlag, Heidelberg, 237-246.
909 Denef, K., Zotarelli, L., Boddey, R.M., Six, J., 2007. Microaggregate-associated
910 carbon as a diagnostic fraction for management-induced changes in soil
911 organic carbon in two Oxisols. Soil Biology and Biochemistry 39(5), 1165-
912 1172.
913 Desanker, P.V., Frost, P.G.H., Frost, C.O., Justice, C.O., Scholes, R.J.e., 1997.
914 Miombo Network: Framework for a Terrestrial Transect Study of Land-Use

915 and Land-Cover Change in the Miombo Ecosystems of Central Africa.
916 Stockholm, Sweden.
917 Desjardins, T., Andreux, F., Volkoff, B., Cerri, C.C., 1994. Organic carbon and ^{13}C
918 contents in soils and soil size-fractions, and their changes due to deforestation
919 and pasture installation in eastern Amazonia. Geoderma 61, 103-118.
920 Diels, J., Vanlauwe, B., Van der Meersch, M.K., Sanginga, N., Merckx, R., 2004.
921 Long-term soil organic carbon dynamics in a subhumid tropical climate: 13C
922 data in mixed C3/C4 cropping and modeling with RothC. Soil Biology and
923 Biochemistry 36(11), 1739-1750.
924 Doorenbos, J., Kassam, A.H., Bentvelsen, C.L.M., Branscheid, V., Plusjé, J.M.G.A.,
925 Smith, M., Uittenbogaard, G.O., Van Der Wal, H.K., 1986. Yield response to
926 water. FAO Irrigation and Drainage Paper 33,
927 Falloon, P., Smith, P., Coleman, K., Marshall, S., 1998. Estimating the size of the
928 inert organic matter pool from total soil organic carbon content for use in the
929 Rothamsted carbon model. Soil Biology and Biochemistry 30, 1207-1211.
930 Falloon, P., Smith, P., Coleman, K., Marshall, S., 2000. How important is inert
931 organic matter for predictive soil carbon modelling using the Rothamsted
932 carbon model? Soil Biology and Biochemistry 32(3), 433-436.
933 Falloon, P., 2001. Large scale spatial modelling of soil organic matter dynamics. PhD
934 Thesis, School of Life and Environmental Sciences, University of Nottingham,
935 UK.
936 Frost, P., 1996. The ecology of miombo woodlands. In: Campbell, B. (Ed.), The
937 Miombo in Transition: Woodlands and Welfare in Africa. CIFOR, Bogor, 11-
938 57.

939 Guo, L.B., Gifford, R.M., 2002. Soil carbon stocks and land use change: a meta
940 analysis. Global Change Biology 8(4), 345-360.
941 Hassink, J., A. P. Whitmore, 1997. A model of the physical protection of organic
942 matter in soils. Soil Science Society of American Journal 61, 131-139.
943 Houghton, R.A., 1999. The annual net flux of carbon to the atmosphere from changes
944 in land use 1850-1990. Tellus B 51, 298-313.
945 Houghton, R.A., 2003. Revised estimates of the annual net flux of carbon to the
946 atmosphere from changes in land use and land management 1850-2000. Tellus
947 B 55(2), 378-390.
948 IPCC, 2007. Climate Change 2007: The Physical Science Basis. Contribution of
949 Working Group I to the Fourth Assessment Report of the Intergovernmental
950 Panel on Climate Change. Solomon, S., Qin, M.M. D., Chen, Z., Marquis, M.,
951 Averyt, K.B., Tignor, M., Miller, H.L. (Eds.), Cambridge University Press,
952 Cambridge, United Kingdom and New York, NY, USA.
953 [Please use the full list of authors, et al.]Janik, L., Spouncer, L., et al., 2002.
954 Sensitivity analysis of the RothC soil carbon model (ver. 26.3 Excel). National
955 Carbon Accounting System Technical Report 30. Australian Greenhouse
956 Office, CSIRO Land and Water and Mathematical and Information Sciences.
957 Canberra, Australia.
958 Jastrow, J.D., Miller, R.M., Boutton, T.W., 1996. Carbon dynamics of aggregate-
959 associated organic matter estimated by carbon-13 natural abundance. Soil
960 Science Society of American Journal 60(3), 801-807.
961 Jenkinson, D.S., 1990. The turnover of organic matter and nitrogen in soil.
962 Philosiophical Transactions: Biological Sciences 329, 361-367.

963 Jenkinson, D.S., Adams, D.E., Wild, A., 1991. Model estimates of CO_2 emissions
964 from soil in response to global warming. Nature 351(6324), 304-306.
965 Jenkinson, D.S., Harkness, D.D., Vance, E.D., Adams, D.E., Harrison, A.F., 1992.
966 Calculating net primary production and annual input of organic matter to soil
967 from the amount and radiocarbon content of soil organic matter. Soil Biology
968 and Biochemistry 24(4), 295-308.
969 Jenkinson, D.S., Hart, P.B.S., Rayner, J.H., Parry, L.C., 1987. Modelling the turnover
970 of organic matter in long-term experiments at Rothamsted. INTECOL Bulletin
971 15, 1-8.
972 Jenkinson, D.S., Meredith, J., Kinyamario, J.I., Warren, G.P., Wong, M.T.F.,
973 Harkness, D.D., Bol, R., Coleman, K., 1999. Estimating net primary
974 production from measurements made on soil organic matter. Ecology 80(8),
975 2762-2773.
976 Jenkinson, D.S., Rayner, J.H., 1977. The turnover of soil organic matter in some of
977 the Rothamsted classical experiments. Soil Science 123(5), 298-305.
978 Jones, P.G., Thornton, P.K., 2000. MarkSim: Software to Generate Daily Weather
979 Data for Latin America and Africa. Agronomy Journal 92(3), 445-453.
980 Kamoni, P.T., Gicheru, P.T., Wokabi, S.M., Easter, M., Milne, E., Coleman, K.,
981 Falloon, P., Paustian, K., Killian, K., Kihanda, F.M., 2007. Evaluation of two
982 soil carbon models using two Kenyan long term experimental datasets.
983 Agriculture, Ecosystems and Environment 122(1), 95-104.
984 Knisel, W. G., 1980. CREAMS: a filed scale model for chemicals, runoff and erosion
985 from agricultural management systems. Conservation Report No. 26.
986 Washington D.C., U.S. Department of Agriculture**,** 640 pp.

987 Lal, R., 2003. Global potential of soil carbon sequestration to mitigate the greenhouse
988 effect. Critical Reviews in Plant Sciences 22, 151-184.
989 Martin, A., Mariotti, A., Balesdent, J., Lavelle, P., Vuattoux, R., 1990. Estimate of
990 organic matter turnover rate in a savanna soil by ^{13}C natural abundance
991 measurements. Soil Biology and Biochemistry 22(4), 517-523.
992 Mitchell, T.D., Jones, P.D., 2005. An improved method of constructing a database of
993 monthly climate observations and associated high-resolution grids.
994 International Journal of Climatology 25(6), 693-712.
995 Molina, J.A.E., Clapp, C.E., Linden, D.R., Allmaras, R.R., Layese, M.F., Dowdy,
996 R.H., Cheng, H.H., 2001. Modeling the incorporation of corn (Zea mays L.)
997 carbon from roots and rhizodeposition into soil organic matter. Soil Biology
998 and Biochemistry 33(1), 83-92.
999 Murty, D., Kirschbaum, M.U.F., Mcmurtrie, R.E., Mcgilvray, H., 2002. Does
1000 conversion of forest to agricultural land change soil carbon and nitrogen? a
1001 review of the literature. Global Change Biology 8(2), 105-123.
1002 New, M., Lister, D., Hulme, M., Makin, I., 2002. A high-resolution data set of surface
1003 climate over global areas. Climate Research 21, 1-25.
1004 Niklaus, P.A., Falloon, P., 2006. Estimating soil carbon sequestration under elevated
1005 CO2 by combining carbon isotope labelling with soil carbon cycle modelling.
1006 Global Change Biology 12(10), 1909-1921.
1007 Paul, S., Veldkamp, E., Flessa, H., 2008. Soil organic carbon in density fractions of
1008 tropical soils under forest - pasture - secondary forest land use changes.
1009 European Journal of Soil Science 59, 359-371.

1010 Running, S.W., Nemani, R.R., Heinsch, F.A., Zhao, M., Reeves, M., Hashimoto, H.,
1011 2004. A continuous satellite-derived measure of global terrestrial primary
1012 production. BioScience 54(6), 547-560.
1013 Schwendenmann, L., Pendall, E., 2006. Effects of forest conversion into grassland on
1014 soil aggregate structure and carbon storage in Panama: Evidence from soil
1015 carbon fractionation and stable isotopes. Plant and Soil 288(1), 217-232.
1016 Shirato, Y., Paisancharoen, K., Sangtong, P., Nakviro, C., Yokozawa, M., Matsumoto,
1017 N., 2005. Testing the Rothamsted Carbon Model against data from long-term
1018 experiments on upland soils in Thailand. European Journal of Soil Science 56,
1019 179-188.
1020 Six, J., Conant, R.T., Paul, E.A., Paustian, K., 2002. Stabilization mechanisms of soil
1021 organic matter: Implications for C-saturation of soils. Plant and Soil 241(2),
1022 155-176.
1023 Six, J., Paustian, K., Elliott, E.T., Combrink, C., 2000. Soil structure and organic
1024 matter: I. distribution of aggregate-size classes and aggregate-associated
1025 carbon. Soil Science Society of Amerian Journal 64, 681-689.
1026 Skjemstad, J.O., Spouncer, L.R., Cowie, B., Swift, R.S., 2004. Calibration of the
1027 Rothamsted organic carbon turnover model (RothC ver. 26.3), using
1028 measurable organic carbon pools. Australian Journal of Soil Research 42, 79-
1029 88.
1030 Smith, B.N., Epstein, S., 1971. Two categories of $^{13}C/^{12}C$ ratios for higher plants.
1031 Plant Physiology 47(3), 380-384.
1032 Smith, J.U., Smith, P., Coleman, K., Hargreaves, P.R., Macdonald, A.J., 2002. Using
1033 dynamic simulation models and the 'Dot-to-Dot' method to determine the

optimum sampling times in field trials. Soil Use and Management 18, 370-375.

Smith, J., Smith, P., 2007. Environmental Modelling. An Introduction. Oxford University Press.

Smith, J., Smith, P., Addiscott, T., 1996. Quantitative methods to evaluate and compare Soil Organic Matter (SOM) models. In: Powlson, D.S., Smith, P., Smith, J. (Eds.), Evaluating Soil Organic Matter Models, 38, NATO ASI series I, Global environmental change. Springer, Berlin-Heidelberg.

Smith, P., Falloon, P., Coleman, K., Smith, J., Piccolo, M.C., Cerri, C.C., Bernoux, M., Jenkinson, D.S., Ingram, J.S.I., Szabó, J., Pástor, L., 2000. Modeling soil carbon dynamics in tropical ecosystems. In: Lal, R., Kimble, J.M., Stewart, B.A. (Eds.), Global climate change and tropical ecosystems. CRC Press, London, 341-364.

Smith, P., Smith, J.U., Powlson, D.S., Coleman, K., Jenkinson, D.S., McGill, W.B., Arah, J.R.M., Thornley, J.H.M., Chertov, O.G., Komarov, A.S., Franko, U., Frolking, S., Li, C., Jensen, L.S., Mueller, T., Kelly, R.H., Parton, W.J., Klein-Gunnewiek, H., Whitmore, A.P., Molina, J.A.E., 1997. A comparison of the performance of nine soil organic matter models using datasets from seven long-term experiments. Geoderma 81(1-2), 153-225.

Sorensen, L.H., 1975. The influence of clay on the rate of decay of amino acid metabolites synthesised in soils during decomposition of cellulose. Soil Biology and Biochemistry 7, 171-177.

Townsend, A.R., Vitousek, P.M., Trumbore, S.E., 1995. Soil organic matter dynamics along gradients in temperature and land use on the Island of Hawaii. Ecology 76(3), 721-733.

1059 Van Oost, K., T. A. Quine, Govers, G., De Gryze, S., Six, J., Harden, J. W., Ritchie, J.
1060 C., McCarty, G. W., Heckrath, G., Kosmas, C., Giraldez, J. V., da Silva, J. R.
1061 Marques, Merckx, R., 2007. The impact of agricultural soil erosion on the
1062 global carbon cycle. Science 318(5850), 626-629.
1063 Van Veen, J.A., Paul, E.A., 1981. Organic carbon dynamics in grassland soils. I.
1064 Background information and computer simulation. Canadian Journal of Soil
1065 Science 61, 185-201.
1066 Vitorello, V.A., Cerri, C.C., Andreux, F., Feller, C., Victória, R.L., 1989. Organic
1067 matter and natural carbon-13 distribution in forested and cultivated oxisols.
1068 Soil Science Society of American Journal 53, 773-778.
1069 Zianis, D., Muukkonen, P., Makipaa, R., Mencuccini, M., 2005. Biomass and stem
1070 volume equations for tree species in Europe. Silva Fennica Monographs 4, 1-
1071 63.
1072 [Please use the full list of authors, et al.]Zimmermann, M., Leifeld, J., et al., 2007.
1073 Measured soil organic matter fractions can be related to pools in the RothC
1074 model. European Journal of Soil Science 58(3), 658-667.
1075 Zingore, S., Manyame, C., Nyamugafata, P., Giller, K.E., 2005. Long-term changes in
1076 organic matter of woodland soils cleared for arable cropping in Zimbabwe.
1077 European Journal of Soil Science 56(6), 727-736.
1078

Figure captions

Figure 1: Measured (squares plus one standard error) and default simulated total C stock changes (solid line) at the four chronosequence sites.

Figure 2: Measured forest derived C (crosses) and maize derived C (squares) and simulated forest derived C (dashed line) and maize derived C (dotted line) at the four chronosequence sites. IOM pool calculated using the model default Falloon equation (Falloon et al., 1998) (dashed-dotted line).

Figure 3: Measured forest derived C (crosses) and simulated forest derived C (dashed line) at the three African chronosequence sites. IOM pool calculated using the model default Falloon equation (a) and IOM pool adjusted to values given by Zingore et al. (2005) (b) (dashed-dotted line).

Figure 4: Measured forest derived C (crosses) and maize derived C (squares) and simulated forest derived C (solid line), simulated forest derived C when accounting for ersion (dashed line), simulated maize derived C (dotted line) and simulated maize derived C when accounting for erosion (dotted line) at Mafungautsi. Please note that dotted lines for the simulation of maize derived C are visually not distinguishable and are therefore plotted in the same style.

Figure 5: Simulated total C (dashed lines) and the sum of the C in the HUM, BIO, DPM and IOM pool (dotted line) for forest and maize derived C, the difference

between the two lines denotes the C in the RPM pool; total C measured (squares) and C in the soil size fraction <50 µm (stars).

Figure 6: Simulated total C (dashed lines), the sum of the C in the silt-humus, clay-humus, BIO, DPM and IOM pool (dotted line) and the sum of C in the clay-humus, BIO, DPM and IOM pool (solid line) for forest and maize derived C, the difference between the dashed and the dotted lines denotes the C in the RPM pool and the difference between the dotted and the solid line denotes the C in the silt-humus pool; total C measured (squares), C in the soil size fraction <50 µm (stars) and C in the soil size fraction 0–2 µm (plus).

Figure 7: RothC model structure after introducing the silt-humus pool

Figure 8: Graphic presentation of the uncertainty analysis results. Solid black lines show average, minimum and maximum simulation curves of 500 simulations. Grey dotted line shows the default simulations. Insets: Histograms depict the distribution of results at the last time step of the simulation at each site, respectively. The grey dotted line shows the default simulation and the grey solid line shows the mean of the distribution.

Tables

Table 1: Model input data

Sites / Parameters	Mafungautsi	Masvingo	Chikwaka	Pyrenean
Clay content (%)	3	9.5	33.5	14.7 (16.1)
Horizon depth (cm)	20	20	20	30
SOC (g C m^{-2})	1950	2540	4190	22173
IOM (g C m^{-2})	144	173	346	2300
Plant input (maize) (g C m^{-2} $year^{-1}$)	12	-[a]	-[a]	500
Months of maize cultivation	November - April	November - April	November – April	June - August

[a] Values are generated by a backwards model run.

Table 2: Ranges of climate data and clay content for uncertainty analysis

	Mafungautsi	Masvingo	Chikwaka	Pyrenean
Yearly mean average temp (ºC)	21.25	20.43	19.07	11.12
Minimum yearly mean average temp (ºC)	20.83	19.39	18.53	10.6
Maximum yearly mean average temp (ºC)	21.5	20.9	19.43	11.6
Yearly mean sum of precipitation (mm)	777.1	636.1	865.7	1092.8
Minimum of yearly sum (mm)	662	610	768.4	934.1
Maximum of yearly sum (mm)	1031	662.2	977.0	1251.5
FAO Soil type	Luvic Arenosol	Hapilic Lixisol	Chromic Luvisol	Vermic Haplumbrept[1]
Mean clay (%)	5.25	10.94	23.66	14.7
Minimum clay (%)	1	4	10	9
Maximum clay (%)	12	18	34	21

[1] US soil taxonomy

Table 3: Results of statistical analysis for default model simulations of maize derived C.

Statistical Parameter	Mafungautsi	Masvingo	Chikwaka	Pyrenean
R	0.69	-0.01	0.73	1.00
RMS **(g C m^{-2})**	21	202	204	610
M **(g C m^{-2})**	-15	127	123	-441

Table 4: IOM values using Falloon-Regression and IOM values of upper and lower 95% confidence interval (C.I.) levels (Falloon et al., 2000).

Site	IOM – 95% C.I. (g C m^{-2})	IOM (g C m^{-2})	IOM + 95% C.I. (g C m^{-2})
Mafungautsi	16	860	1335
Masvingo	18	800	1681
Chikwaka	29	1430	4079
Pyrenean	113	2300	46700

Table 5: Results of statistical test for the simulation of forest and maize derived C at the Pyrenean site using the implementation of the silt-humus pool

Statistical Parameter	Total forest C	Silt forest C	Clay forest C	Total maize C	Silt maize C	Clay maize C
R	1.00[1]	1.00[1]	0.86	0.99	0.99	0.99
RMS **(g C m^{-2})**	398	1506	2067	147	129	66
M **(g C m^{-2})**	-144	-1488	-1698	-110	52	-10

Table 6: Summary of descriptive statistics of the uncertainty analysis results for forest and maize plant input values

Site	Forest plant input (g C m^{-2} year^{-1})			Maize plant input (g C m^{-2} year^{-1})		
	Average	Min	Max	Average	Min	max
Mafungautsi	165	148	186	10	9	11
Masvingo	176	154	204	35	30	41
Chikwaka	266	232	305	68	59	79
Pyrenean	899	744	1103	-	-	-

Figures

Figure 1

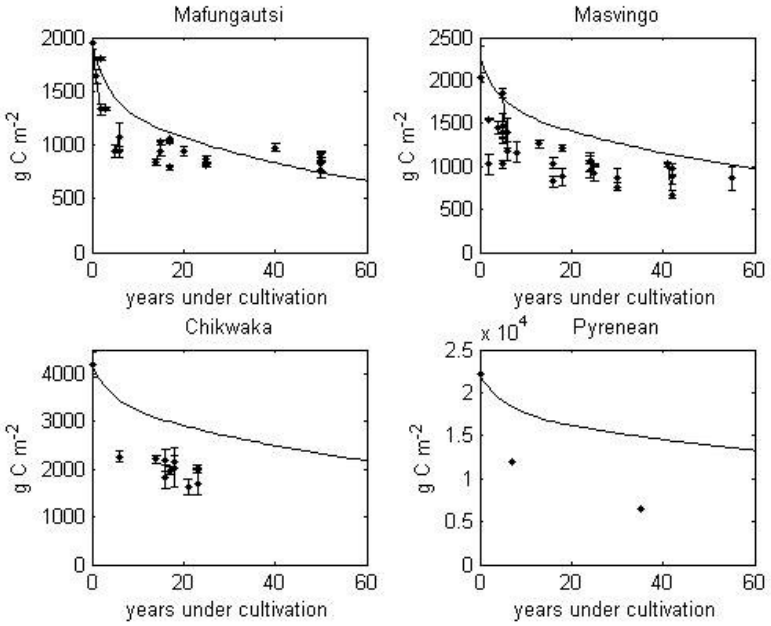

Figure 2

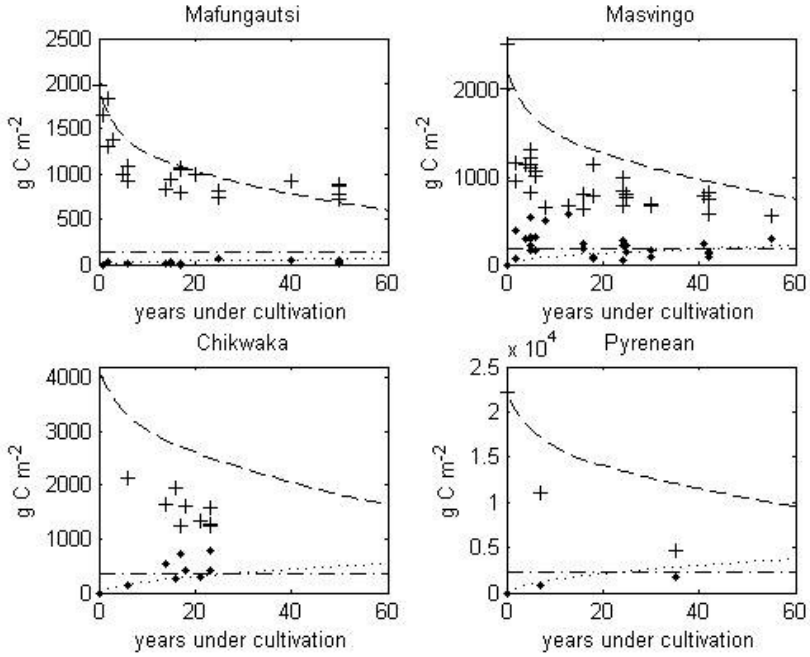

Figure 3

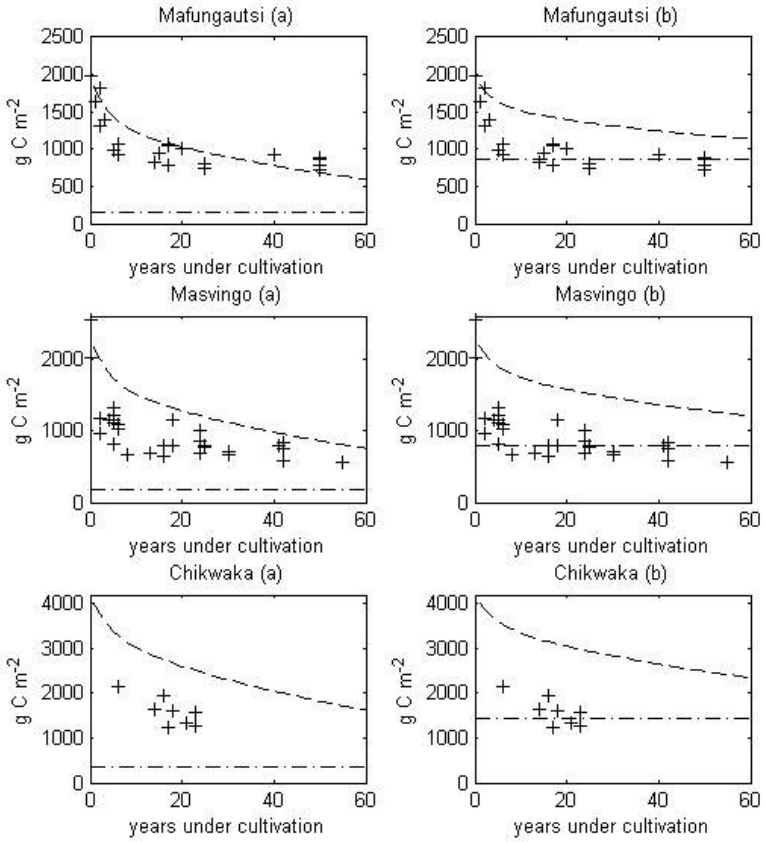

Figure 4

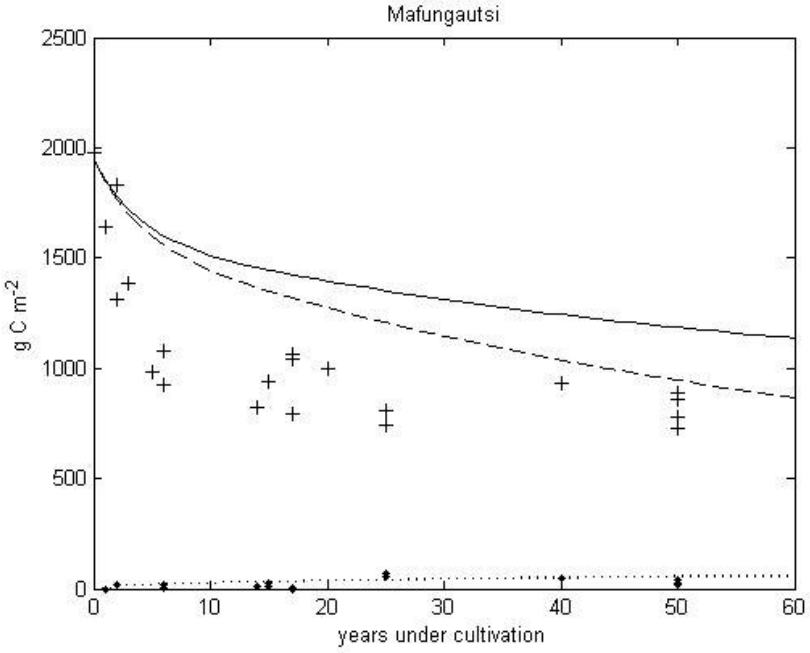

Figure 5

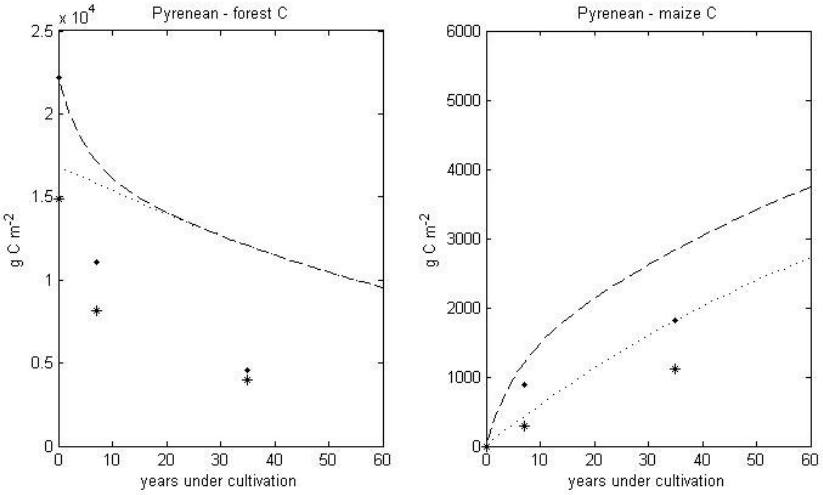

Figure 6

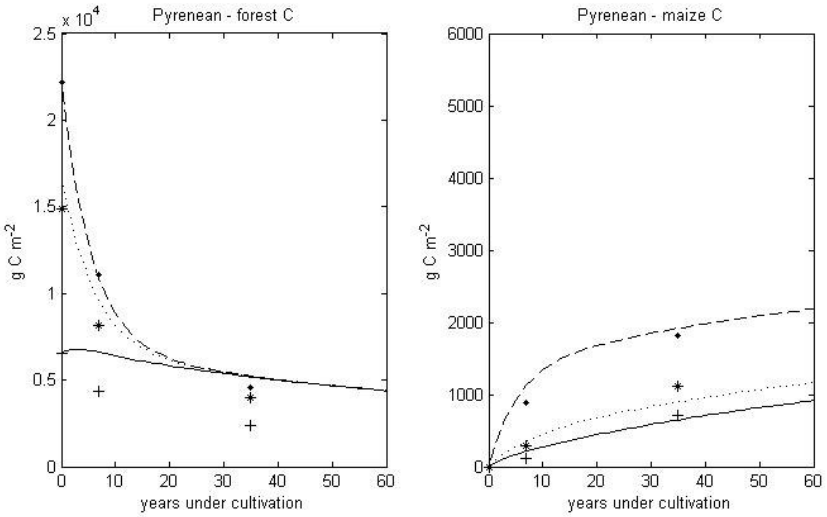

Figure 7

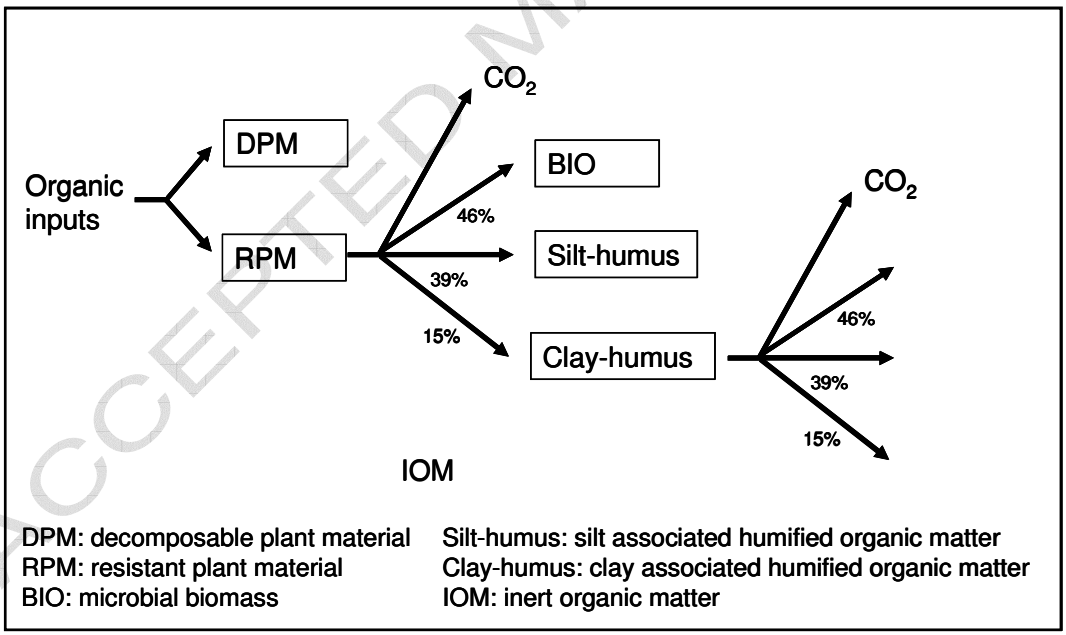

Figure 8